Exploring the Protective Effects of *Bellucia dichotoma* Cong. Aqueous Extract on Spleens Following *Bothrops atrox* Envenomation in Mice: A Stereological Investigation

ABSTRACT

The aqueous extract of *Bellucia dichotoma* (AeBd) has traditionally been used in cases of snakebites and has been shown to be promising against the effects of *Bothrops atrox* venom (BaV). There is evidence of local venom blocking action by AeBd in envenomed mice; however, studies of the systemic action of this plant against BaV are lacking. Antibothropic serum (ABS) is the conventional therapy after envenomation by *B. atrox*. The association of AeBd and ABS can also be an alternative for the patient. As an organ capable of initiating the innate and adaptive defense, the spleen is a sensor of the body's immune status. Via stereology, this study evaluated the mouse spleen when challenged with the venom of *B. atrox*, as well as the role of AeBd (alone or in association with ABS) as an alternative treatment for *Bothrops* envenomations. In this study, male Swiss mice were divided into five groups: control, BaV, AeBd, AeBd/ABS, and ABS. After 24 h, the spleens were removed and set in plastic resin according to the norms of stereology to produce 9-13 sections/organ. Red (RP) and white pulp (WP) represented 67-75 % and 22-29 %, respectively, in all groups. Spleen volume was reduced in BaV due to decreased RP and WP (PALS). The number of macrophages was increased in BaV in relation to the other groups (from 2.289 ± 301 in the control to 3.807 ± 494 cells.mm^{-2}). No changes were detected in the numbers of lymphocytes and megakaryocytes. In conclusion, the aqueous extract of *B. dichotoma* administered orally shortly after a *B. atrox* envenomation was effective in inhibiting morphological alterations in the spleen of the mice. The association AeBd/ABS maintains the same venom blocking effectiveness, thus showing that the use of this traditional therapy (AeBd) by local populations can be effective in inhibiting the systemic effects caused by *B. atrox* envenomations.

Keywords: *Bothrops atrox*, *Bellucia dichotoma*, aqueous extract, herbal medicine, spleen, stereology.

Introduction

Bites caused by snakes are considered a serious public health problem and, every year, they cause thousands of deaths or serious sequelae in the victims. In 2017, the World Health Organization added snakebites to the list of neglected tropical diseases, estimating that annually 1.8-2.7 million people are envenomated by snakes worldwide, resulting in between 81,000 and 138,000 deaths and 400,000 survivors with permanent sequelae (Longbottom et al., 2018; Williams et al., 2010). In Brazil, an estimated 26,000 cases of snakebite envenoming occur every year. Many of the victims are rural workers, fishers, extractivists, indigenous people or other groups who live in close proximity to the forest (Schneider et al., 2021). The northern region of the country has the highest incidence of cases per 100,000 inhabitants (Zemero et al., 2023).

Most of the envenomations that occur in the Amazon region are attributed to the species *Bothrops atrox*, popularly known as the jararaca, white-tailed jararaca, surucucurana and jipoboia (Cardoso et al., 2009; Waldez and Vogt, 2009; Wen et al., 2015). The venom of this snake has a hemolytic, edematous and necrotizing effect. The use of antiophidic serum is the conventional therapy for treating injured victims; however, access to this type of treatment in most cases, is a privilege of the population living close to urban centers. In the Amazon, great distances separate the native population from this the centers that provide this type of treatment, and this is the reason why the use of alternative treatments with natural or herbal products is so widespread (Bochner et al., 2014; Waldez and Vogt, 2009).

Medicinal plants are frequently used in folk medicine around the world as pre- and post-treatments against envenomations by snakes. *Bellucia dichotoma* Cogn. is a species that is endemic to the Amazon region and, in Brazil, it is found in the states of Acre, Amazonas, Amapá and Pará, and is popularly known as muúba or goiaba-de-anta (Baumgratz, 2013). The population uses the bark to prepare a tea before entering the forest, as a preventive measure and it is also given to victims after snakebite. The main classes of substances found in the aqueous extract of *B. dichotoma* bark are fatty acids, flavonoids, terpenes, hydrolyzable and condensed tannins (Moura et al., 2013). This

extract has already been shown to be effective in inhibiting the hemorrhagic, phospholipasic, edematogenic and coagulant effects in rats after envenomation by *Bothrops jararaca* and *B. atrox* snakes (Moura et al., 2015; Moura et al., 2013). In mice, the aqueous extract of *B. dichotoma*, given orally as traditionally used, significantly reduced paw edema in the first 30 minutes after *B. atrox* envenomation and its full anti-edematogenic action was observed after 6 hours of treatment (Moura et al., 2014). More positive results were obtained with the simultaneous use of the extract (orally) and antibothropic serum (intravenously) (Moura et al., 2014). These results are promising for the protective effect of the *B. dichotoma* extract in other sites, such as the spleen, for example.

The spleen is the largest secondary lymphoid organ and is responsible for immune surveillance, immune response to circulating antigens, hematopoiesis, and blood filtration (Cesta, 2006; Mebius and Kraal, 2005; Steiniger, 2015). The splenic parenchyma is divided into white and red pulp. The white pulp is responsible for initiating immune responses to blood antigens, as it contains a quarter of the body's lymphocytes and has other phagocytic cells that are important in the immune response (*e.g.*, macrophages, neutrophils and dendritic cells). The white pulp is composed of a periarteriolar lymphoid sheath that is rich in T lymphocytes (PALS), follicles (B lymphocytes) and a marginal zone (B lymphocytes) (Cesta, 2006). Macrophages are categorized into different subsets based on their location, function, and phenotype. Blood arriving in the spleen via the splenic artery follows two parallel paths: the closed/rapid circulation (inside vessels such as the central arterioles and their branches surrounded by the PALS of the white pulp) and then follows through post-sinusoid venules that converge in the splenic vein; the open/slow circulation goes through the splenic cords and sinuses of the red pulp where macrophages and reticular cells filter the blood cells before they return to the general circulation. Defective cells and antigens are phagocytosed by macrophages or dendritic cells (Steiniger, 2015).

Several studies have shown that alterations occur in the spleen after snake envenomations and the subsequent use of medicinal plants (Almeida et al., 2020; Goorani et al., 2020; Zangeneh, 2020). Pathological alterations indicate congestion, hemorrhage, extramedullary hematopoiesis and necrosis in the most severe cases (Raposo et al., 2000; Silva et al., 2012; Venkatesan et al., 2014). Thus, this study quantitatively evaluated the spleen morphology of mice challenged with *Bothrops atrox*

venom, as well as the role of the extract of *Bellucia dichotoma* (alone or in association with antibothropic serum) in the preservation of splenic components.

Materials and methods

Experimental animals

Male Swiss mice (N=17, 34-41 g) obtained from the Animal Facility of the Federal University of Oeste do Pará (UFOPA), Santarém, Pará, Brazil were used. This study was approved by the Ethics Committee on the use of Animals at the University of the State of Pará (UEPA/Protocol 43/11), Santarém, Pará, Brazil. The animals were maintained in standard cages at a temperature of 22 ± 1 ºC, in a 12 h light/12 h dark cycle, with water and feed *ad libitum*.

Acquisition of *Bothrops atrox* venom and antibothropic serum

The venom was obtained by squeezing the glands of adult *Bothrops atrox* (Linnaeus, 1758) (Viperidae) snakes obtained in the Tapajós National Forest (FLONA), located at km 83 of the BR-163 highway, in Santarém, Pará, Brazil. Both the collection of the snake and the extraction of the venom were permitted by the Chico Mendes Institute for Biodiversity Conservation (ICMBio), via the Biodiversity Authorization and Information System (SISBIO – No. 14018). The venom was collected, then lyophilized and kept at -20 ^{o}C until use (permission to keep snakes in the vivarium of Faculdades Integradas do Tapajós (FIT), Santarém, PA, was obtained from the National Council for Control of Animal Experiments - CONCEA No. 26/2013). In this study, the antibothropic serum (ABS) produced by Instituto Butantan, São Paulo, Brazil, (batch number: 105113B) was used.

Aqueous extract of the bark of *Bellucia dichotoma*

The aqueous extract of the bark of *B. dichotoma* (Melastomataceae) (AeBd) was prepared in accordance with the methods used bt the residents of the Eixo Forte communities in the western region of Pará, Amazon, Brazil (Access to associated

traditional knowledge, process No. 01450.008934/2014-68-DPI/IPHAN). In summary, 50 g of powdered *B. dichotoma* bark was diluted in distilled water (1:10) maintained at a constant temperature of 100 ^{o}C. After cooling, 150 mL was removed, which is the equivalent to a cup of tea, as used locally. This was then lyophilized and the final dry weight of the extract obtained was 2.9 g.

Experimental design

The mice were randomly distributed in standard cages and submitted to one of the following treatments for 24 h: Control – subplantar injection of 0.9% saline solution (n=3); BaV – *B. atrox* venom injection (5 µg, equivalent to two minimal edematogenic doses). The venom was injected into the footpad of the right hind paw of the mice in a constant volume of 50 µL (n=4); AeBd – oral administration of aqueous extract of *B. dichotoma* (283.30 mg/kg), immediately after injection of *B. atrox* venom (n=3); AeBd/ABS – AeBd + antibothropic serum (ABS) via ophthalmic venous plexus (100 µL), after injection of *B. atrox* venom (n=3); ABS – injection of antibothropic serum (ABS) via ophthalmic venous plexus (100 µL), after injection of *B. atrox* venom (n=4).

Spleen removal and volumetry

After 24 hours, the animals were sacrificed by displacement of the cervical spine and the spleen was removed, which was then weighed on an analytical balance (Shimadzu AY220, Japan) and fixed in buffered formalin for 48 hours.

Two procedures were adopted to determine the absolute volume of the spleen: (i) fluid displacement (Scherle, 1970) and (ii) serial sections according to the Cavalieri principle (Howard and Reed, 2005). The Cavalieri principle is described in the stereological section. Both approaches allow one to obtain the absolute volume, but they differ in terms of precision and accuracy of results and in terms of their practicality of application. In the first approach, the intact organs were individually submerged in a container with the same fixative solution using a thin copper wire (Fig. 1A). The organ was fully immersed in the solution, but without touching the bottom and sides of the container. The set was then placed on an analytical balance (Shimadzu AY220, Japan).

Before immersion, the balance was reset and the value observed on the electronic panel after immersion represented the organ volume without fluid density correction (Scherle, 1970). For density correction, the following equation was used: $\boldsymbol{V = \frac{W}{\rho}}$, where **V**, organ volume; **W**, weight of the immersed organ and **ρ** is the density of the fluid (formaldehyde solution = 1.060 g.cm^3).

Histological processing and stereology

The spleens were cut in half and the systematic, uniform and random orientation was obtained using the orientator (Mattfeldt et al., 1985). This procedure allows one to obtain sections with high variability in the arrangements of structure profiles, which ensures a reduction in the sampling bias. Then, the spleens were dehydrated in increasing concentrations of ethanol (70 and 96%), pre-infiltrated with 96% ethanol/plastic resin, placed in individual molds and infiltrated with hydroxyethyl-methacrylate plastic resin (Technovit 7100, Külzer-Heraues, Germany). The molds were left in a heated oven at 40 ºC for 24 h for the complete polymerization of the resin (Fig. 1B). The total length of the two halves in the resin block was determined and this value divided by 9-13, depending on the length of the spleen (Fig. 1B). The microtomy was then performed (Leica RM 2145, Germany). The sections were stained with 0.5% Toluidine Blue (Toluidine Blue, 0.12 g; Na^+ borate, 0.5g; distilled H_2O, 100 mL; for 30 seconds) and Basic Fuchsin (Basic Fuchsin, 0.5 g and distilled H_2O, 100 mL; for 2 seconds) and then photographed (magnification at 100x) under a light microscope (Leica DM4B, Germany). A grid was superimposed on each image containing points generated using the Imod software (version 4.7/stereology module) (Kremer et al., 1996). The analysis consists of counting random points that are overlaid on the image; those that touch the spleen are counted (Fig. 1C).

The volume of the spleen was determined by: $\boldsymbol{V_{spleen} = \sum_{i=1}^{m} Pi \times T \times \frac{a}{p}}$, where, $\boldsymbol{\sum Pi}$ is the total number of points on each spleen, $\boldsymbol{\frac{a}{p}}$ is the area represented by each point (44,100 μm^2) and **T** (1,000 μm) is the distance between each serial section. An error limit of 5% was considered acceptable (Gundersen and Østerby, 1981).

The percentage of internal components (volume density) was obtained using Delesse's principle (Howard and Reed, 2005). A magnification of 400x was used in the randomly selected fields of view, which were photographed under a light microscope (Leica DM4B, Germany) (Fig. 1D). The percentage of volume occupied by each component in relation to the reference space (splenic parenchyma) was calculated using following equation: $\boldsymbol{Vv} = \frac{\sum_{i=1}^{m} \boldsymbol{Pcomp}}{\sum_{i=1}^{m} \boldsymbol{Pref}}$), where **Vv** is the volume density of a given component (red pulp, RP; periarteriolar lymphoid sheath, PALS; follicles; marginal zone, MZ; trabecula; capsule) and ***Pref*** is the sum of points that touch the reference space. The white pulp (WP) represented the sum of PALS + follicles + MZ. The percentages obtained for each component were transformed into absolute volume by being multiplied using the Cavalieri volume:

$$\boldsymbol{Absolute\ volume}\ (\boldsymbol{mm^3}) = \boldsymbol{Vv\ x\ Cavalieri\ Volume}\ (\boldsymbol{mm^3})$$

Number of cell profiles

A two-dimensional quantification was used to determine the number of profiles of megakaryocytes, lymphocytes and macrophages in the marginal zone. For this, a grid containing four lines delimiting a counting frame was used (Fig. 2). The technique consists of counting the cell nuclei contained in the counting system. The following equation was used:

$$\boldsymbol{Q} = \frac{\sum \boldsymbol{Q}}{(\sum \boldsymbol{Nframes} \times \sum \boldsymbol{Aframe})}$$

Where: $\sum \boldsymbol{Q}$ is the number of cell profiles; $\sum \boldsymbol{Nframes}$ is the sum of analyzed frames and $\sum \boldsymbol{Aframe}$ is the frame area $(261 \times 10^{-6}\ mm^2)$.

Statistical analysis

The Prism program (GraphPad Software, Inc., CA, USA) was used for the statistical and graphical analysis of this study. Data were tested for normality using the Kolmogorov-Smirnov test and analyzed using one-way ANOVA. In cases in which the difference between groups is indicated, Tukey's parametric test of multiple comparisons was used to compare the mean values between the experimental groups. The confidence limit established for the tests was 5%. The stereological data obtaining from serial sections were evaluated for each spleen volume and the variance estimator was determined using the coefficient of error according to Cruz-Orive (1999):

$$\mathbf{CE} = \left[\mathbf{0.0724} \times \frac{\boldsymbol{B}}{\sqrt{\boldsymbol{A}}} \times \frac{\sqrt{\boldsymbol{n}}}{(\sum_{\boldsymbol{i=1}}^{\boldsymbol{m}} \boldsymbol{Pi})^{\frac{3}{2}}}\right]^{\frac{1}{2}}$$, where: CE indicates the coefficient of error, $\frac{\boldsymbol{B}}{\sqrt{\boldsymbol{A}}}$ indicates the variance of the cross-sectional areas (shape coefficient) and depends on the complexity of the structures; **n** represents the number of evaluated sections and $\sum_{\boldsymbol{i=1}}^{\boldsymbol{m}} \boldsymbol{Pi}$ is the number of points counted in the sections.

Results

There was no significant difference in the spleen volume when measured using the Cavalieri principle and when using fluid displacement (Fig. 3A). The higher values obtained using fluid displacement may be related to the presence of extra splenic tissues that increase the total volume of the organ. The RP was the most representative component in all the treatments (67-75%), followed by WP (22-29%), capsule (0.8-2.9%) and trabecula (0.7-1.0%) (Fig. 3B).

The spleen mass and the spleen/body mass ratio showed a non-significant decrease in the BaV group (Fig. 4A and B). The spleen volume (Cavalieri, mm^3 kg^{-1}) was reduced in the BaV group compared to the other treatments (Fig. 4C). The decrease in the volume of red pulp (Fig. 4D) in the BaV group compared to the control and white pulp (Fig. 4E), in relation to the other treatments, explains the reduction in splenic volume. PALS was reduced in the BaV group (Fig. 4F). No changes were observed in the follicles (Fig. 4G) or in the marginal zone (Fig. 4H). Neither were there any changes in the trabecular connective component (Fig. 4I), but the capsule was increased in AeBd/ABS group in relation to the BaV group (Fig. 4J).

The number of macrophages was increased in the marginal zone of the BaV group when compared to the other treatments (Fig. 5A). There was no significant difference in the number of lymphocytes in the same region (Fig. 5B) or in megakaryocytes in the red pulp (Fig. 5C). The structural morphology of the spleen was maintained in all treatments. The spleen presented a typical structure with a distinct red and white pulp (Fig. 5D). Splenic cords were seen bordering splenic sinusoids in the red pulp. The white pulp presented well-defined PALS delimited by a marginal zone bordering the red pulp (Fig. 5E). Megakaryocytes were frequently were observed in the red pulp.

Figure 6 shows the interaction between the components of the spleen and their relationship with the total volume of the organ. In this interpretation, it is possible to observe the relative distance between the BaV group and the others. This treatment was characterized by a smaller volume of white and red pulp, resulting in a smaller volume of the spleen. The AeBd and AeBd/ABS groups showed comparable effect to the control and the ABS.

Figure 7A-E shows the influence of the number of sections on the accuracy of the volume determination using the Cavalieri principle. The spleen volume in the different treatments starts to stabilize after the 12^{th} serial section. However, a coefficient of error below 5% can already be observed from the 6^{th} section onwards. These results indicate that efficiency and precision in this study were achieved with 12 histological sections. Less is imprecise, more is inefficient.

Discussion

Antiophidic therapy based on popular knowledge is widely used to alleviate the damage caused by snakebites in the Amazon. *Bellucia dichotoma* is traditionally used as an antidote for snakebites and for various other ailments. Our study revealed that the acute action of BaV reduced the volume of RP and WP, specifically by reducing PALS, thus contributing to the reduction in spleen volume. Furthermore, snake venom increased the number of macrophages in MZ. The extract of *B. dichotoma* inhibits the effects of *Bothrops atrox* venom, and preserves the splenic microstructures and probably the spleen's function. The combination of the extract of *B. dichotoma* and the antibothropic serum has the same splenic protective effect.

The spleen histology of the animals in this study is seen to be in agreement with the literature (Cesta, 2006). The spleen volume of the mice (34-41 g), in this study assessed by point counting on serial sections (40-58 mm^3, Cavalieri volume) and by fluid displacement (49-90 mm^3), is in accordance with the volume specified by optical contrast CT (44 -61 mm^3) on six-week-old female Balb/c mice (McErlean et al., 2015) and by stereology (35 mm^3, Cavalieri volume) on Balb/c male mice (25-30 g) (Vojdani et al., 2010).

Approximately 75% of the spleen is RP (Fig. 3B), which consists of connective tissue, arterioles, capillaries, sinusoids, venules and blood cells (Steiniger, 2015). The reduction of RP in the BaV group, and probably the impairment of the filtering/hematopoietic function of the spleen, may be associated with (i) the hemolytic action of metalloproteinases and serineproteases (Gutiérrez, 2002) associated with the effect of an impairment of the filtering/hematopoietic function by the consumption of endogenous fibrinogen that exacerbates the hemorrhagic condition (Gutiérrez, 2002; Gutiérrez and Rucavado, 2000) and (ii) the direct action of the venom on the splenic structure causing cell death. In the study by Navarro et al. (2014), *Crotalus atrox* venom (0.5-1.0 μg, peritoneal injection) showed direct cytocidal activity in the splenocytes of CD-1 mice (females, 6-8 weeks old, 20-25 g), in addition to an increase in the expression of inflammatory cytokines.

Snake venoms cause hemorrhage, congestion, autophagy, splenomegaly and, rarely, necrosis of the spleen (Raposo et al., 2000; Silva et al., 2012; Venkatesan et al., 2014). An analysis of the paws inoculated with the venom revealed a high percentage of hemorrhage (unpublished data), which indicates the action of proteases in coagulopathy, cytotoxicity (especially phospholipases A_2) and in the degradation of the components of the extracellular matrix of the vessels, which promotes the extravasation of blood cells to adjacent tissues. Under such circumstances, a state of splenomegaly (as mentioned before), with increased red pulp as an indication of activation of extramedullary hematopoiesis and antigen filtration, is common (Silva et al., 2012). Our results are in opposition to this scenario possibly due to the acute aspect of the envenomation protocol employed. These observations suggest that damage to the spleen is progressive after venom inoculation and that in the first 24 h after the inoculation morphological alterations are less severe. A similar condition was reported by Moreno and Gutiérrez (1988), whereby the spleens of mice envenomed by *Bothrops asper* showed no significant histological alterations in the RP after 24 h. More severe alterations such as congestion and splenic hemorrhage have been reported in horses after *Bothrops* sp envenomations (>24 h) (Raposo et al., 2000).

The *Bothrops* venom was responsible for the reduction in PALS and, consequently, for the decrease in the volume of WP, possibly due to its cytotoxic action (Fig. 4E-F). WP is responsible for initiating immune responses to blood antigens, as it contains a quarter of the body's lymphocytes, in addition to other important phagocytic

cells (macrophages, neutrophils, and dendritic cells). These alterations can affect lymphocyte trafficking and the plasma cell development that takes place in PALS. The increase in BaV macrophages may be related to phagocytosis of toxic compounds from the venom and cell debris from cell death. Macrophage activation is directly related to the production of pro-inflammatory cytokines (Cesta, 2006). Increased numbers of splenic follicular macrophages were also observed in rabbits after envenomation by *Vipera raddei*, an indication of moderate inflammation and complement system activation (Aznaurian and Amiryan, 2006).

Our results showed that the combination of AeBd/ABS promoted a significant increase in the splenic capsule, possibly providing greater physical protection to the organ against rupture. The dense fibroelastic nature and the presence of smooth muscle cells in the capsule make it a tough yet flexible scaffold enabling contraction and release of blood cells into the circulation (Kai et al., 2000). However, recent studies indicate that, although mouse splenic capsules are extensively innervated, there is no evidence that they can contract, as occurs in rats (Seifert and Offner, 2018) and humans (Lodin-Sundström and Schagatay, 2010). The role of catecholaminergic innervation appears to be related to controlling immune cell death (Lodin-Sundström and Schagatay, 2010). In our study, the trabeculae in the AeBd/ABS group also showed an increase, although it was not statistically significant. The lowest mean values for the capsule, seen in the AeBd group, should be the focus of future investigations.

A number of extracts and their isolated compounds have been evaluated for their antiophidic capacity (Félix-Silva et al., 2017; Fung et al., 2009; Gopi et al., 2015). In our study, the AeBd and AeBd/ABS treatments were effective in preserving splenic components. A possible explanation lies in the ability of the aqueous extract of the bark of *B. dichotoma* to block the activity of phospholipases A_2 or PLA_2 (Moura et al., 2013) and metalloproteinases Zn^{++}/dependent (Moura et al., 2014). The blocking action of the extract are believed to be related to the presence of polyphenolic compounds and tannins that precipitate the venom proteins and form a complex with Zn^{++} and Ca^{++}, which inhibits the enzymatic activity (Moura et al., 2014; Moura et al., 2013).

In several recent studies, stereology has been used to investigate the medicinal value of plants traditionally used in folk medicine. The study by Jena et al. (2016) showed the protective role of *Prunus africanus* in benign prostatic hyperplasia in rats. *Allium sativum* and *Nigella sativa* also protected the duodenal mucosa of chickens

(Aydogan et al., 2020). CCl_4 hepatotoxicity was reduced in mice treated with *Sophora alopecuroides* (Doorgard and Pournaghi, 2018). The use of stereology for investigating the effect of plant extracts on the spleen has shown that *Spinacia oleracea* (nanocapsules) reduces myeloblast infiltration in leukemic mice (Zangeneh, 2020), *Allium eriophyllum* (nanocapsules) plays an immunoprotective role on the white and red pulp during hemolytic anemia in mice (Goorani et al., 2020) and *Athenaea velutina* increases red pulp (improving hematopoiesis) in cancer-induced mice (Almeida et al., 2020). In our study, stereology was efficient and accurate for determining the total volume of the spleen and its components. The use of 9-13 sections obtained throughout the organ was sufficient in order to determine the volumes, with an error of below 5%. These data support the precision of our analysis and make it clear that the use of few (< 6) and non-serial sections is highly risky and may compromise the study, leading the researcher to draw erroneous conclusions based on the obtained quantifications.

conclusion : this study showed that the aqueous extract of *B. dichotoma*, administered orally soon after inoculation with *B. atrox* venom, had a splenic-protective effect. The association of the extract with the antibothropic serum maintains the same blocking effectiveness, thus showing that the use of this therapy, which is used by local populations, can be effective in inhibiting the local (Moura et al., 2014; Moura et al., 2017) and systemic effects caused by *B. atrox* venom. The future of snakebite envenoming therapy holds promise for more effective, accessible, and affordable treatments through advances in technology, research, and public health strategies (Laustsen et al., 2016).

Declaration of interest

The authors declare that they have no known competing financial interests or personal relationships that could have appeared to influence the work reported in this paper.

Acknowledgments

This article represents the master's dissertation presented by MBA to the Post-graduate Program in Basic and Applied Immunology at the Federal University of Amazonas

(UFAM). The authors are grateful to Erilene Carmo dos Santos (UFAM) for her invaluable help with the histotechnological processing.

Funding

Financial support was provided in the form of grants from Fundação de Amparo à Pesquisa do Estado do Amazonas (FAPEAM) (POSGRAD Program #005/2022 and #002/2023), Conselho Nacional de Desenvolvimento Científico e Tecnológico (CNPq) and Coordenação de Aperfeiçoamento de Pessoal de Nível Superior (CAPES) (PDPG-CONSOLIDACAO-3-4 Program #88887.707248/2022-00). The funders had no role in the study design, data collection and analysis, decision to publish, or the preparation of the manuscript.

References

Almeida, A. A., Lima, G. D., Simão, M. V., Moreira, G. A., Siqueira, R. P., Zanatta, A. C., Vilegas, W., Machado-Neves, M., Bressan, G. C. and Leite, J. P. (2020). Screening of plants from the Brazilian Atlantic Forest led to the identification of *Athenaea velutina* (Solanaceae) as a novel source of antimetastatic agents. *Int. J. Exp. Pathol.* **101**, 106-121.

Aydogan, I., Yildirim, E., Kurum, A., Bolat, D., Cinar, M., Basalan, M. and Yigit, A. (2020). The effect of dietary darlic (*Allium Sativum*), black cumin (*Nigella Sativa*) and their combination on performance, intestine morphometry, serum biochemistry and antioxidant status of broiler chickens. *Braz. J. Poult. Sci.* **22**.

Aznaurian, A. V. and Amiryan, S. V. (2006). Histopathological changes induced by the venom of the snake Vipera raddei (Armenian adder). *Toxicon* **47**, 141-143.

Baumgratz, J. F. A. (2013). Lista de espécies da flora do Brasil: *Bellucia dichotoma*: Jardim Botânico do Rio de Janeiro.

Bochner, R., Fiszon, J. T. and Machado, C. (2014). A profile of snake bites in Brazil, 2001 to 2012. *Journal of Clinical Toxicology* **4**, 1-7.

Cardoso, J. L. C., França, F. O. S., Wen, F. H., Málaque, C. M. S. and Haddad Jr., V. (2009). Animais peçonhentos no Brasil: biologia, clínica e terapêutica dos acidentes. São Paulo: Servier.

Cesta, M. F. (2006). Normal structure, function, and histology of the spleen. *Toxicol. Pathol.* **34**, 455-465.

Cruz-Orive, L. M. (1999). Precision of Cavalieri sections and slices with local errors. *J. Microsc.* **193**, 182-198.

Doorgard, E. and Pournaghi, P. (2018). The ameliorative potential of *Sophora alopecuroides* essential oil on CCl4-induced hepatotoxicity in mice; a stereological study. *Res.J. Pharmacogn.* **5**, 47-54.

Félix-Silva, J., Gomes, J. A., Xavier-Santos, J. B., Passos, J. G., Silva-Junior, A. A., Tambourgi, D. V. and Fernandes-Pedrosa, M. F. (2017). Inhibition of local effects induced by Bothrops erythromelas snake venom: Assessment of the effectiveness of Brazilian polyvalent bothropic antivenom and aqueous leaf extract of Jatropha gossypiifolia. *Toxicon* **125**, 74-83.

Fung, S., Tan, N., Liew, S., Sim, S. and Aguiyi, J. (2009). The protective effects of *Mucuna pruriens* seed extract against histopathological changes induced by *Malayan cobra* (*Naja sputatrix*) venom in rats. *Trop. Biomed.* **26**, 80-84.

Goorani, S., Koohi, M. K., Morovvati, H., Hassan, J., Ahmeda, A. and Zangeneh, M. M. (2020). Application of natural compounds–based gold nanoparticles for the treatment of hemolytic anemia in an anemic mouse model: Formulation of a novel drug from relationship between the nanotechnology and hematology sciences. *Appl. Organomet. Chem.* **34**, e5475.

Gopi, K., Renu, K., Vishwanath, B. S. and Jayaraman, G. (2015). Protective effect of *Euphorbia hirta* and its components against snake venom induced lethality. *J. Ethnopharmacol.* **165**, 180-190.

Gundersen, H. and Østerby, R. (1981). Optimizing sampling efficiency of stereological studies in biology: or 'Do more less well!'. *J. Microsc.* **121**, 65-73.

Gutiérrez, J. M. (2002). Comprendiendo los venenos de serpientes: 50 años de investigaciones en América Latina. *Rev. Biol. Trop.* **50**, 377-394.

Gutiérrez, J. M. and Rucavado, A. (2000). Snake venom metalloproteinases: Their role in the pathogenesis of local tissue damage. *Biochimie* **82**, 841-850.

Howard, C. V. and Reed, M. G. (2005). Unbiased stereology: three-dimensional measurement in microscopy. New York, Berlin, Heidelberg: Springer-Verlag.

Jena, A. K., Vasisht, K., Sharma, N., Kaur, R., Dhingra, M. S. and Karan, M. (2016). Amelioration of testosterone induced benign prostatic hyperplasia by Prunus species. *J. Ethnopharmacol.* **190**, 33-45.

Kai, T., Nishizono, H. and Kimura, K. (2000). Fiber arrangement of the rat splenic capsule with special reference to elastic fibers. *Okajimas Folia Anat. Jpn.* **77**, 167-179.

Kremer, J. R., Mastronarde, D. N. and McIntosh, J. R. (1996). Computer visualization of three-dimensional image data using IMOD. *J. Struct. Biol.* **116**, 71-76.

Laustsen, A. H., Engmark, M., Milbo, C., Johannesen, J., Lomonte, B., Maria Gutierrez, J. and Lohse, B. (2016). From fangs to pharmacology: the future of snakebite envenoming therapy. *Curr. Pharm. Des.* **22**, 5270-5293.

Lodin-Sundström, A. and Schagatay, E. (2010). Spleen contraction during 20 min normobaric hypoxia and 2 min apnea in humans. *Aviat. Space Environ. Med.* **81**, 545-549.

Longbottom, J., Shearer, F. M., Devine, M., Alcoba, G., Chappuis, F., Weiss, D. J., Ray, S. E., Ray, N., Warrell, D. A. and de Castañeda, R. R. (2018). Vulnerability to snakebite envenoming: a global mapping of hotspots. *The Lancet* **392**, 673-684.

Mattfeldt, T., Möbius, H. J. and Mall, G. (1985). Orthogonal triplet probes: an efficient method for unbiased estimation of length and surface of objects with unknown orientation in space. *J. Microsc.* **139**, 279-289.

McErlean, C. M., Boult, J. K., Collins, D. J., Leach, M. O., Robinson, S. P. and Doran, S. J. (2015). Detecting microvascular changes in the mouse spleen using optical computed tomography. *Microvasc. Res.* **101**, 96-102.

Mebius, R. E. and Kraal, G. (2005). Structure and function of the spleen. *Nat. Rev. Immunol.* **5**, 606-616.

Moreno, E. and Gutiérrez, J. (1988). Body distribution of Bothrops asper (terciopelo) snake venom myotoxin and its relationship to pathological changes. *Toxicon* **26**, 403-409.

Moura, V. M., Bezerra, A. N. S., Mourão, R. H. V., Lameiras, J. L. V., Raposo, J. D. A., Sousa, R. L., Boechat, A. L., Oliveira, R. B., Chalkidis, H. M. and Dos-Santos, M. C. (2014). A comparison of the ability of *Bellucia dichotoma* Cogn. (Melastomataceae) extract to inhibit the local effects of *Bothrops atrox* venom when pre-incubated and when used according to traditional methods. *Toxicon* **85**, 59-68.

Moura, V. M., Sousa, L. A. F., Dos-Santos, M. C., Raposo, J. D. A., Lima, A. E., Oliveira, R. B., Silva, M. N. and Mourão, R. H. V. (2015). Plants used to treat snakebites in Santarém, western Pará, Brazil: An assessment of their effectiveness in inhibiting hemorrhagic activity induced by *Bothrops jararaca* venom. *Journal of Ethnopharmacology* **161**, 224-232.

Moura, V. M., Sousa, L. A. F., Oliveira, R. B., Silva, A. M. M., Chalkidis, H. M., Silva, M. N., Pacheco, S. and Moura, R. H. V. (2013). Inhibition of the principal enzymatic and biological effects of the crude venom of *Bothrops atrox* by plant extracts. *Journal of Medicinal Plants Research* **7**, 2330-2337.

Moura, V. M. d., de Souza, L. Y. A., da Costa Guimarães, N., Dos Santos, I. G. C., de Almeida, P. D. O., de Oliveira, R. B., Mourão, R. H. V. and Dos-Santos, M. C. (2017). The potential of aqueous extracts of *Bellucia dichotoma* Cogn.(Melastomataceae) to inhibit the biological activities of *Bothrops atrox* venom: A comparison of specimens collected in the states of Pará and Amazonas, Brazil. *J. Ethnopharmacol.* **196**, 168-177.

Navarro, L. B., Gonzalez-Clara, F., Arteaga-Figueroa, L., Mendonça, R. Z. and Petricevitch, V. (2014). Effect of crotalus atrox venom on peritoneal and spleen cell and mediators production. *International Journal of Pharmacy and Pharmaceutical Sciences*, p. 323-8.

Raposo, J. B., del Carmen Méndez, M., Baialardi, C. E. G. and Raffi, M. B. (2000). Acidente ofídico em eqüino no sul do Brasil-Relato de caso. *Revista da FZVA* **7**.

Scherle, W. (1970). A simple method for volumetry of organs in quantitative stereology. *Mikroskopie* **26**, 57.

Schneider, M. C., Min, K.-d., Hamrick, P. N., Montebello, L. R., Ranieri, T. M., Mardini, L., Camara, V. M., Raggio Luiz, R., Liese, B. and Vuckovic, M. (2021). Overview of snakebite in Brazil: Possible drivers and a tool for risk mapping. *PLOS Neglected Tropical Diseases* **15**, e0009044.

Seifert, H. A. and Offner, H. (2018). The splenic response to stroke: from rodents to stroke subjects. *Journal of Neuroinflammation* **15**, 1-7.

Silva, A., Gunawardena, P., Weilgama, D., Maduwage, K. and Gawarammana, I. (2012). Comparative in-vivo toxicity of venoms from South Asian hump-nosed pit vipers (Viperidae: Crotalinae: Hypnale). *BMC research notes* **5**, 471.

Steiniger, B. S. (2015). Human spleen microanatomy: why mice do not suffice. *Immunology* **145**, 334-346.

Venkatesan, C., Sarathi, M., Balasubramanian, G., Thomas, J., Balachander, V., Babu, V. S., Bilal, S. M. Y., Majeed, S. A., Madan, N. and Raj, N. S. (2014). Antivenom activity of triterpenoid (C34H68O2) from Leucas aspera Linn. against Naja naja naja venom induced toxicity: Antioxidant and histological study in mice. *Human & experimental toxicology* **33**, 336-359.

Vojdani, Z., Dehghani, F., Seyedi, F., Nourafshan, A. and Baha, A. B. F. (2010). Quantitative study of the effects of morphine on the mouse spleen and inguinal lymph node. *Archives of Iranian Medicine* **13**, 294-300.

Waldez, F. and Vogt, R. C. (2009). Aspectos ecológicos e epidemiológicos de acidentes ofídicos em comunidades ribeirinhas do baixo rio Purus, Amazonas, Brasil. *Acta Amazon.* **39**, 681-696.

Wen, F. H., Monteiro, W. M., da Silva, A. M. M., Tambourgi, D. V., da Silva, I. M., Sampaio, V. S., dos Santos, M. C., Sachett, J., Ferreira, L. C. L. and Kalil, J. (2015). Snakebites and scorpion stings in the Brazilian Amazon: identifying research

priorities for a largely neglected problem. *PLoS Neglected Tropical Diseases* **9**, e0003701.

Williams, D., Gutiérrez, J. M., Harrison, R., Warrell, D. A., White, J., Winkel, K. D. and Gopalakrishnakone, P. (2010). The Global Snake Bite Initiative: an antidote for snake bite. *The lancet* **375**, 89-91.

Zangeneh, M. M. (2020). Green synthesis and formulation a modern chemotherapeutic drug of *Spinacia oleracea* L. leaf aqueous extract conjugated silver nanoparticles; Chemical characterization and analysis of their cytotoxicity, antioxidant, and anti-acute myeloid leukemia properties in comparison to doxorubicin in a leukemic mouse model. *Appl. Organomet. Chem.* **34**, e5295.

Zemero, M. I. M., Christino, M. G. and Franco, M. C. A. (2023). Acidentes com animais peçonhentos na região Norte do Brasil na série histórica de 2007–2017. *Pará Research Medical Journal* **68**.

Figure Legends

Figure 1. A. Direct determination of volume using fluid displacement on an analytical balance. **B.** Application of the Cavalieri principle by counting points on the serial sections. Organs were sectioned in halves, set in plastic resin and oriented randomly. The total length of the two halves (L1 and L2) was added and divided by 9-13 (equivalent to the number of sections to be obtained). **C.** Counting system containing crosses superimposed on each of the sections. A magnification of 100x was used to increase counting accuracy. For this, the counting system was moved along the entire section (in this example, 10 points are countable). The area denoted as x/y in the counting system indicates the area per point (a/p = 44,100 μm^2), an essential factor for transforming points into volume. **D.** Diagram of the randomly selected field seen at higher magnification with details of the counting system for determining the percentage of components in the spleen using the Delesse principle.

Figure 2. A. Diagram of the spleen region superimposed with a counting system containing a frame of defined dimensions. This system was used for counting megakaryocyte profiles (m1, m2 and m3), lymphocytes and macrophages. The system has solid lines (permitted line) and dashed lines (exclusion line). If the nucleus of the cell in question is seen within the frame or touching the continuous line, it is counted (*e.g.*, m2 and m3). However, if the nucleus is outside the frame or touches the dashed line, it is not counted (*e.g.*, m1). **B.** Counting system with defined area for counting lymphocytes and macrophages. Red pulp, RP; white pulp, WP; MZ, marginal zone.

Figure 3. A. Spleen volume determined using the Cavalieri principle (left) and fluid displacement (right). Data in mm^3. **B.** Percentage of splenic components. Red pulp, RP; white pulp, WP; trabecula, TRA; capsule, CAP.

Figure 4. Biometrics and stereology (absolute volumes). **A.** Spleen mass. **B.** Spleen mass and body mass ratio. **C.** Cavalieri volume. **D.** Red pulp volume, RP. **E.** White pulp volume, WP. **F.** Periarteriolar lymphoid sheath volume, PALS. **G.** Follicle volume. **H.** Marginal zone volume, MZ**. I.** Trabecula volume. **J.** Capsule volume. Statistical difference indicated (One-way ANOVA, Tukey test).

Figure 5. Cell number and histology. **A.** Macrophages. **B**. Lymphocytes. **C.** Megakaryocytes. **D.** Red pulp. Top detail: entire section of the spleen revealing its main components. Lower detail: megakaryocytes. **E.** White pulp. CAP, capsule; TRA, trabecula; RP, red pulp; WP, white pulp; FL, follicle; PALS, periarteriolar lymphoid sheath; MZ, marginal zone; SC, splenic cords; SS, splenic sinusoids. Statistical difference indicated (One-way ANOVA, Tukey test).

Figure 6. Trilinear diagram of the interaction between the major components of the spleen. Note the separation between the BaV group and the other treatment groups.

Figure 7. Effect of increasing the number of serial sections on Cavalieri volume and coefficient of error. **A.** Control. **B**. BaV. **C.** AeBd. **D.** AeBd/ABS. **E.** ABS. Increasing the number of sections reduces the CE of the analysis, bringing the volume closer to a stability plateau. Solid lines = volume. Dashed lines = coefficient of error (CE).

Figure 1.

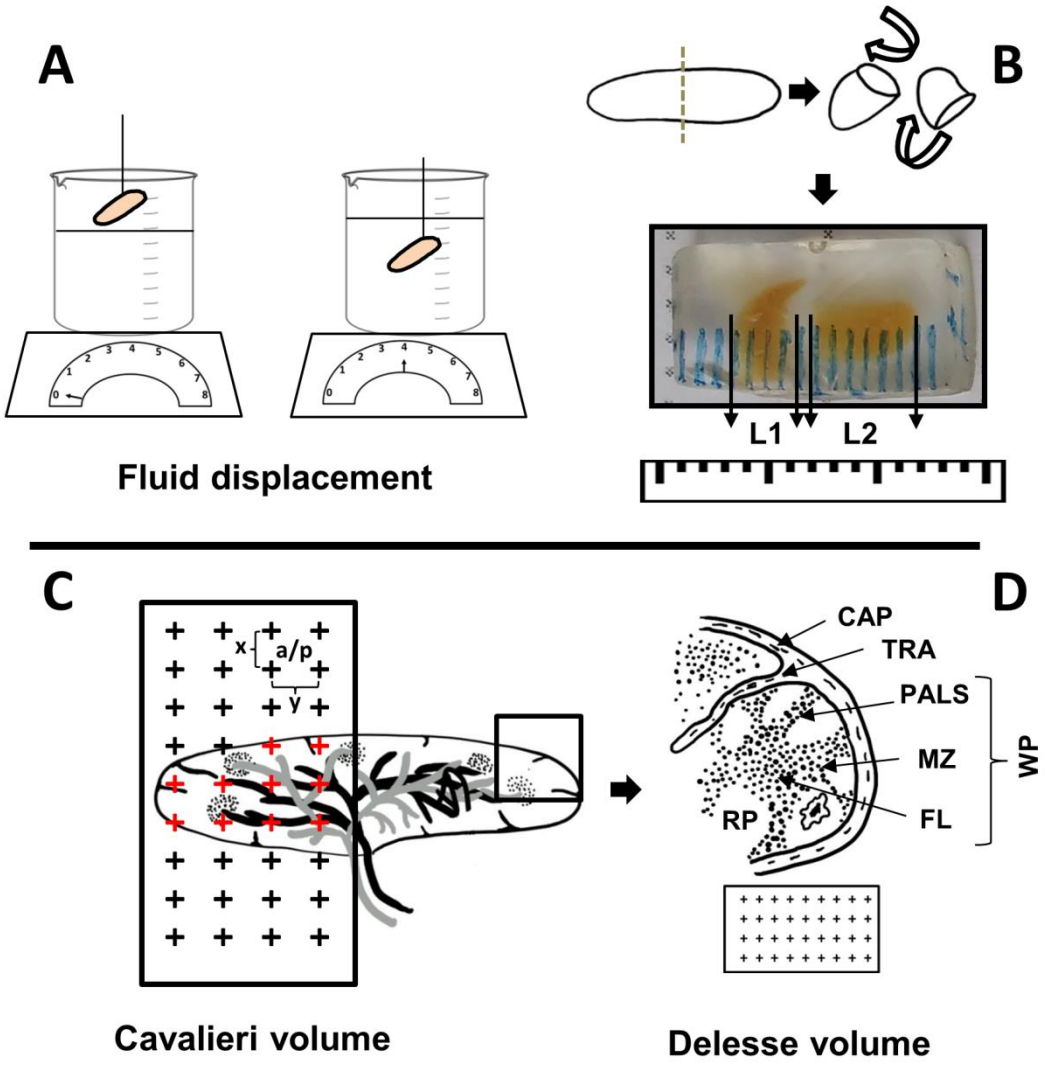
A
B
L1
L2
Fluid displacement
C
D
x
a/p
y
CAP
TRA
PALS
MZ
RP
FL
WP
Cavalieri volume
Delesse volume

1 **Figure 2.**

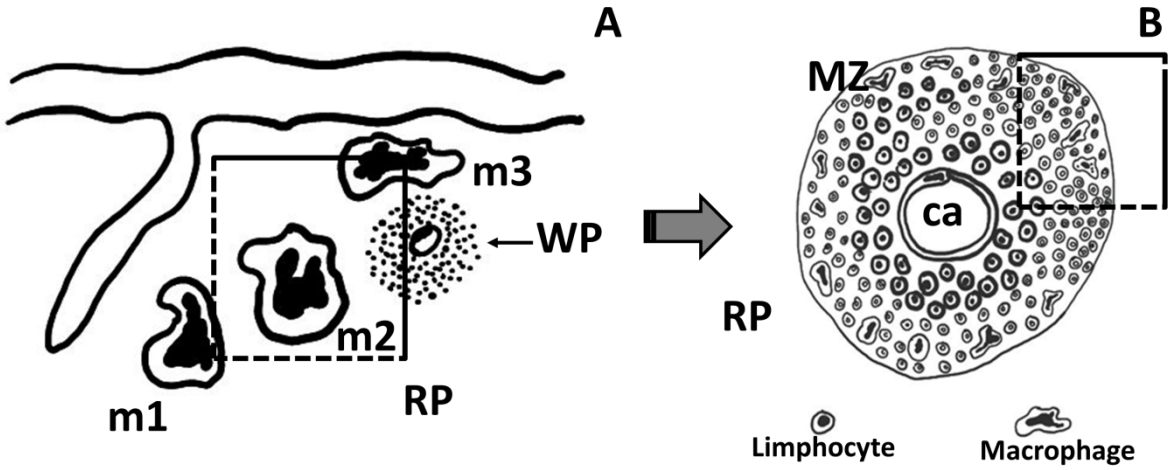

2
3

Figure 3.

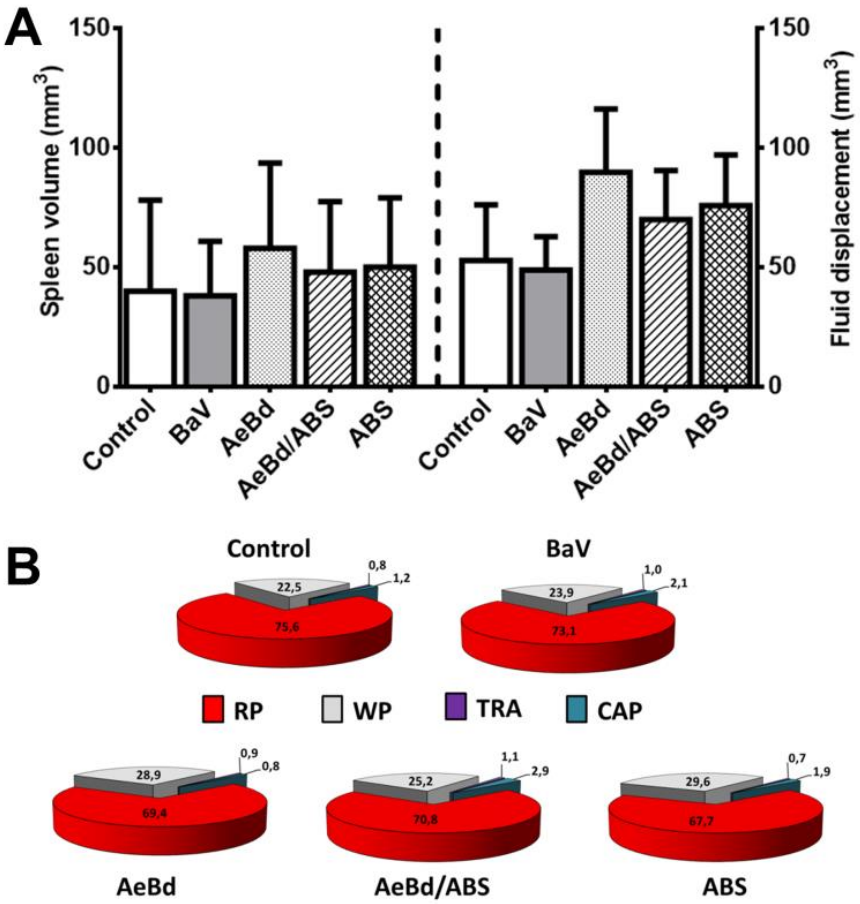
A
Spleen volume (mm3)
Fluid displacement (mm3)
150
100
50
0
Control
BaV
AeBd
AeBd/ABS
ABS
B
Control
BaV
22,5
0,8
1,2
75,6
23,9
1,0
2,1
73,1
RP
WP
TRA
CAP
28,9
0,9
0,8
69,4
25,2
1,1
2,9
70,8
29,6
0,7
1,9
67,7
AeBd
AeBd/ABS
ABS

Figure 4.

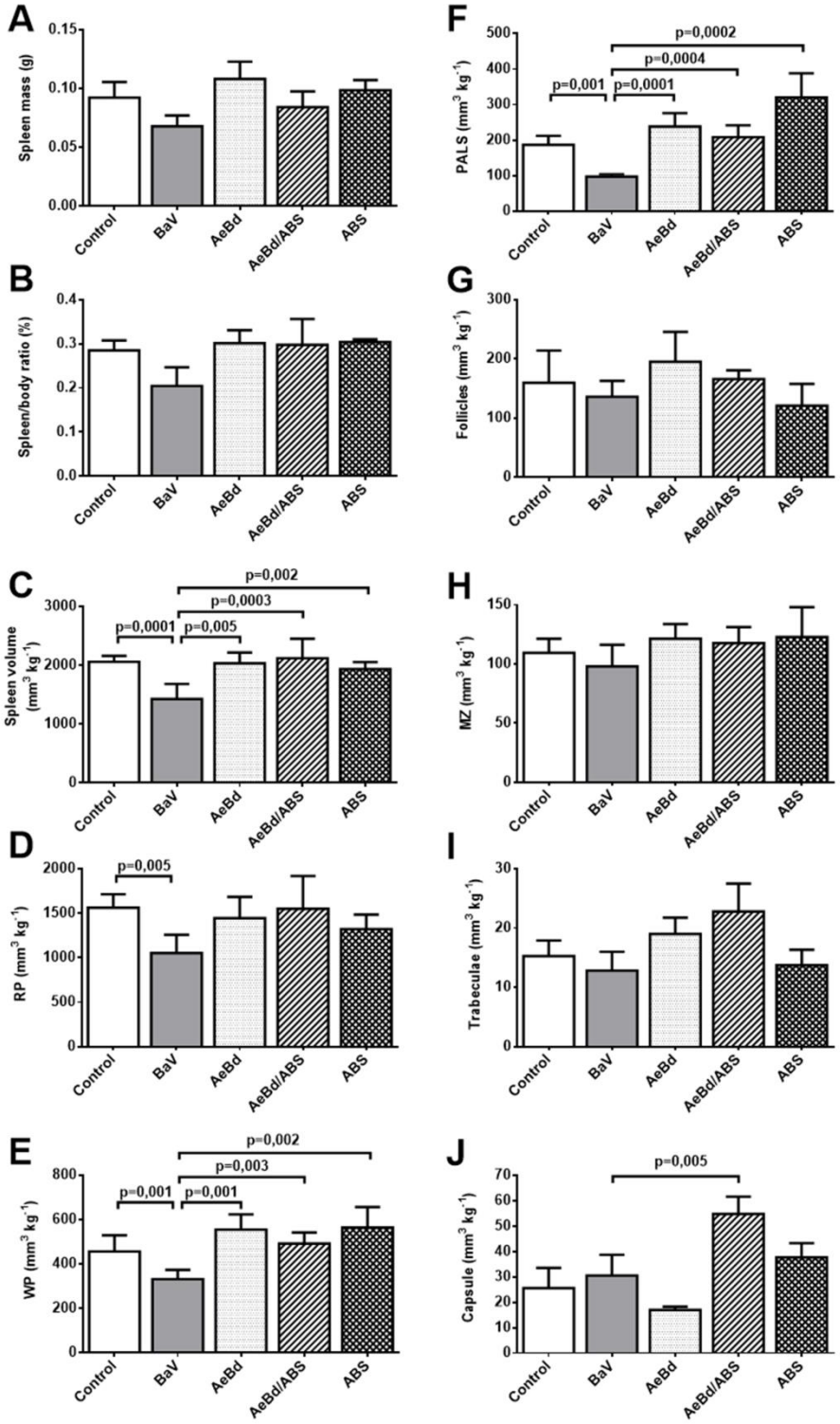
A
Spleen mass (g)
0.15
0.10
0.05
0.00
Control
BaV
AeBd
AeBd/ABS
ABS
B
Spleen/body ratio (%)
0.4
0.3
0.2
0.1
0.0
C
Spleen volume (mm3 kg-1)
3000
2000
1000
0
p=0,002
p=0,0003
p=0,0001
p=0,005
D
RP (mm3 kg-1)
2000
1500
1000
500
0
p=0,005
E
WP (mm3 kg-1)
800
600
400
200
0
p=0,002
p=0,003
p=0,001
p=0,001
F
PALS (mm3 kg-1)
500
400
300
200
100
0
p=0,0002
p=0,0004
p=0,001
p=0,0001
G
Follicles (mm3 kg-1)
300
200
100
0
H
MZ (mm3 kg-1)
150
100
50
0
I
Trabeculae (mm3 kg-1)
30
20
10
0
J
Capsule (mm3 kg-1)
70
60
50
40
30
20
10
0
p=0,005

Figure 5.

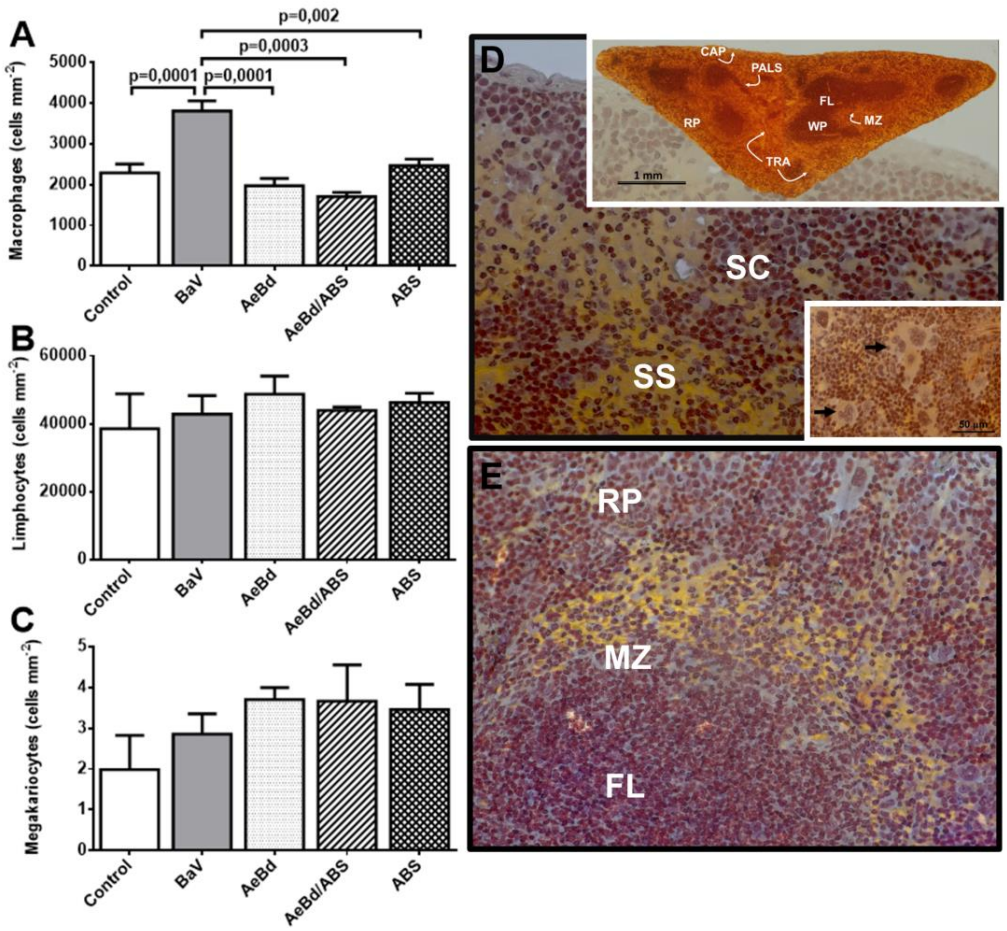
A
Macrophages (cells mm-2)
p=0,002
p=0,0003
p=0,0001
p=0,0001
5000
4000
3000
2000
1000
0
Control
BaV
AeBd
AeBd/ABS
ABS
B
Limphocytes (cells mm-2)
60000
40000
20000
0
C
Megakariocytes (cells mm-2)
5
4
3
2
1
0
D
CAP
PALS
FL
RP
WP
MZ
TRA
1 mm
SC
SS
50 µm
E
RP
MZ
FL

Figure 6.

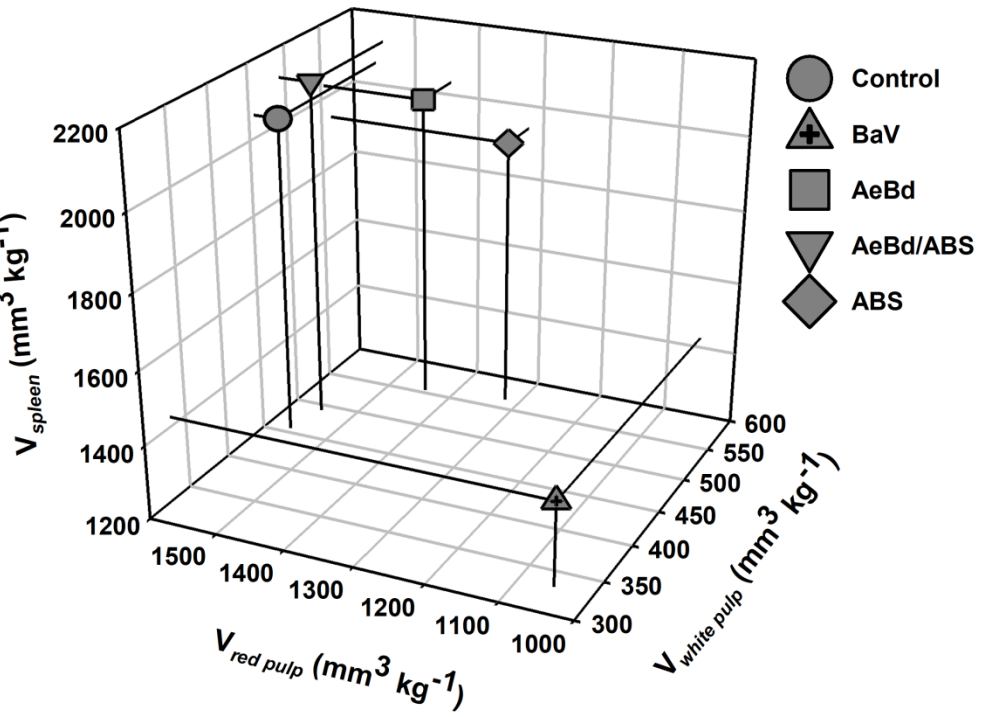
Control
BaV
AeBd
AeBd/ABS
ABS
2200
2000
1800
1600
1400
1200
V spleen (mm3 kg-1)
1500
1400
1300
1200
1100
1000
V red pulp (mm3 kg-1)
600
550
500
450
400
350
300
V white pulp (mm3 kg-1)

Figure 7.

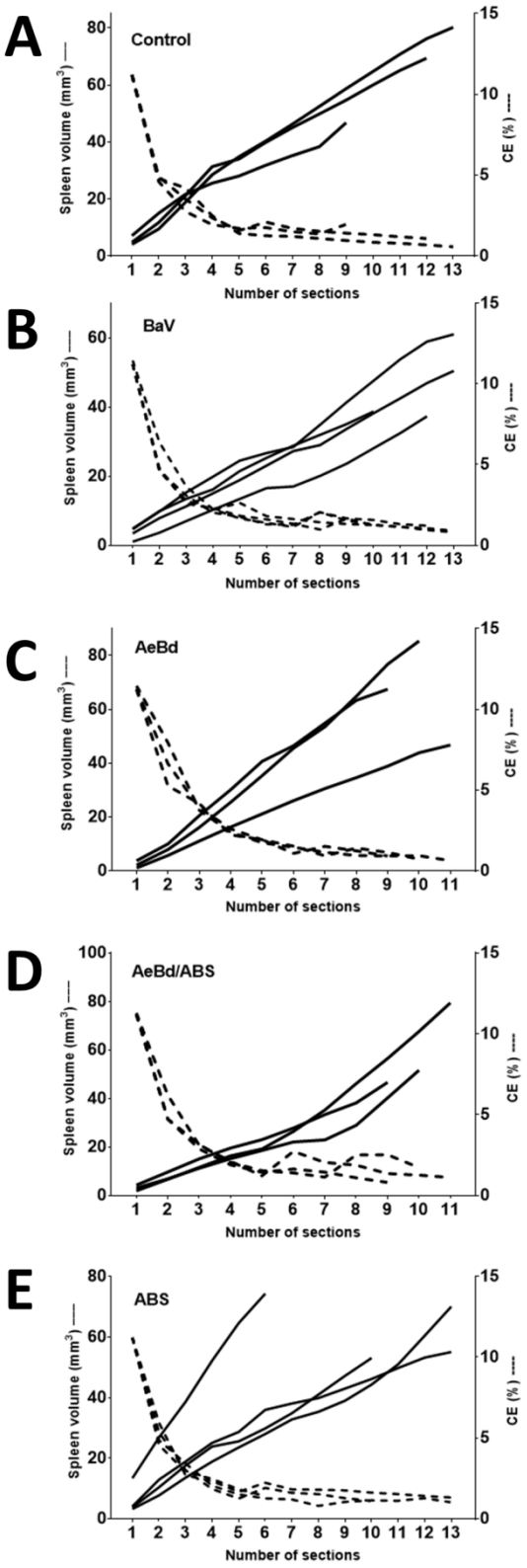
A
Control
B
BaV
C
AeBd
D
AeBd/ABS
E
ABS
Spleen volume (mm³) —
CE (%) ----
Number of sections